# Self-Assembly of Poly(diethylhexyloxy-*p*-phenylenevinylene)-*b*-poly(4-vinylpyridine) Rod−Coil Block Copolymer Systems

**Nicolas Sary,[†] Laurent Rubatat,[†] Cyril Brochon,[‡] Georges Hadziioannou,[‡] Janne Ruokolainen,[§] and Raffaele Mezzenga*,[⊥,†]**

*Department of Physics and Fribourg Center for Nanomaterials, University of Fribourg, Ch. Musée 3, CH-1700, Fribourg, Switzerland; Laboratoire d'Ingénierie des Polymères pour les Hautes Technologies, UMR 7165, Université Louis Pasteur, Ecole Européenne de Chimie, Polymères et Matériaux, 25, Rue Becquerel, 67087 Strasbourg, France; Physics Laboratory, Helsinki University of Technology, Helsinki 02015, Finland; and Nestlé Research Center, Vers-Chez-Les-Blanc, 1000 Lausanne 26, Switzerland*

ABSTRACT: We describe the synthesis, the morphology, and self-assembly behavior of semiconducting poly(4-vinylpyridine-*b*-diethylhexyloxy-*p*-phenylenevinylene) (P4VP-*b*-PPV) rod−coil block copolymer systems. Three different block copolymers with 55%, 80%, and 88% coil volume fraction were synthesized by convergent anionic polymerization in THF using lithium α-methylstyrene as initiator. The morphology of the block copolymers was studied by transmission electron microscopy, small-angle X-ray scattering, and small-angle neutron scattering as a function of the volume fraction of the rod block as well as different annealing conditions. The microphase-separated morphologies in these block copolymers vary from lamellar, to hexagonal, and spherical, when the volume fraction of the rod is progressively reduced. By combining the lattice parameter measured by scattering techniques with the volume fraction of rod domains obtained by nuclear magnetic resonance, it was shown that the block copolymers in the lamellar structure are organized in a smectic C double layer, while in the hexagonal phase they self-organize in a homeotropic arrangement, with the rod blocks forming the dispersed phase. Furthermore, while self-assembly of rod−coil block copolymers in columnar hexagonal phase prevents close rod packing, for the lamellar phase evidence of this configuration among rods is shown by wide-angle X-ray scattering. As a consequence, the morphology and long-range order in the lamellar phase are the result of simultaneous inter-rods liquid crystalline interactions and the tendency to microphase segregation of rod and coil. As a result, depending on temperature, the lamellar phase can exist both with rods oriented in a smectic configuration and with randomly packed rods. We show that annealing the lamellar phase below its order−disorder transition temperature, $T_{ODT}$, but above the maximum affordable temperature for inter-rods liquid crystalline interactions, called smectic-in-lamellar to lamellar order−disorder transition temperature, $T_{SL}$ (with $T_{SL} < T_{ODT}$), leads to highly improved long-range lamellar order, which is then preserved when the system is cooled below $T_{SL}$, at which temperature rod close packing is fully recovered.



## Introduction

The field of self-assembly of diblock and multiblock copolymers with flexible coil blocks is well established and has been the subject of extensive studies for more than 45 years. More recently, the field of block copolymers has been expanding, including new classes of polymers with unconventional molecular architectures, including the presence of rigid blocks, which provide liquid crystalline behavior to the polymers.[1−3] While the mechanisms leading to spherical, hexagonal, bicontinuous gyroid, or lamellar phases in coil−coil block copolymers are well understood,[4−6] phase separation in rod−coil block copolymers remains more debated.[7,8] The phase and self-assembly behaviors of these polymers are further complicated by the fact that the rigidity of the rod block can be achieved by either forming α-helices in polypeptides or by the delocalization the $\pi$-electron clouds in the case of $\pi$-conjugated polymers. This may introduce in the self-assembly driving force intermolecular rod−rod interactions such as hydrogen-bonding or $\pi-\pi$ interactions, respectively. In particular, the effect of $\pi-\pi$ interactions in the self-assembly of mesoscopic systems has been already demonstrated in discotic liquid crystals and rod−coil block copolymers.[9−11] Furthermore, unlike coil−coil block copolymers which are composed of two blocks exhibiting similar conformations, the assembly of rod and coil blocks to form a single polymer chain induces strong conformational asymmetry and thus original phase separation properties and mechanisms.[12] An increasing number of experimental studies have been carried out during the past 10 years, enabled by remarkable advances in the synthesis of rod−coil block copolymers. Two main approaches for the synthesis of $\pi$-conjugated rod−coil block copolymers have been developed: the divergent path consists of the living polymerization of the coil block started from a rod macroinitiator,[13−15] whereas in the convergent way the coil block obtained by living polymerization is linked, either quenched[16−18] or condensated,[19−23] with the end-functionalized rod. An alternative route, however, restricted to some particular polymers, consists of successively polymerizing by living anionic polymerization two coil blocks where one is a precursor for the rod.[24] In the present work, the quenching of living anionic polymerization of the 4-vinylpyridine is used to synthesize poly(diethylhexyloxy-*p*-phenylenevinylene)-*b*-poly(4-vinylpyridine) block copolymers (PPV-*b*-P4VP).

* To whom correspondence should be addressed: e-mail raffaele.mezzenga@unifr.ch, Tel + 41 26 300 9066, Fax + 41 26 300 9747; e-mail raffaele.mezzenga@rdls.nestle.com, Tel + 41 21 785 8078, Fax + 41 21 785 8554.
[†] University of Fribourg.
[‡] Université Louis Pasteur.
[§] Helsinki University of Technology.
[⊥] Nestlé Research Center.

These specific rod−coil block copolymers systems are then employed to study the self-assembly behavior of rod−coil block copolymers in the presence of inter-rod liquid crystalline interactions. In the PPV-*b*-P4VP copolymers under study, the rod and coil blocks have a stronger tendency toward phase segregation than previously investigated analogous PPV-*b*-polystyrene block copolymers.[9] Furthermore, this system is also relevant as a promising component for photovoltaic devices.[25] Indeed, recent work has demonstrated the possibility of forming poly(4-vinylpyridine)/fullerene (P4VP:$C_{60}$) complexes, thus enabling the use of P4VP as a chaperone matrix for hosting electron acceptor $C_{60}$ molecules and the design of PPV-*b*-P4VP:$C_{60}$ with large electron donor/electron acceptor interfaces[26] which are believed to be essential for the dissociation into charges of the excitons forming upon light exposure.[27] However, in order to fully exploit these systems for efficient optoelectronic applications, continuous percolating mesophases such as lamellar, cylindrical, or gyroidal must be designed, controlled, and used. These structures have already been observed in various rod−coil block copolymers: Stupp et al. reported formation of lamellar and hexagonal phase-separated domains for various rod to coil volume fractions in monodisperse rod−coil diblock copolymers,[28] whereas lamellar and bicontinuous liquid crystalline assemblies as well as hexagonal columnar phase are observed in rod−coil−rod triblock copolymers.[29] The emphasis of the present work is placed on the study of the synthesis, design, and self-assembly mechanisms of PPV-*b*-P4VP block copolymers, with particular accent on morphologies exhibiting continuous domains, such as hexagonal and lamellar, of possible use as templates in organic photovoltaic devices.

## Experimental Section

**Materials**. *sec*-Butyllithium (1.4 M in hexane), used as initiator for anionic polymerization, was purchased from Aldrich. 4-Vinylpyridine (Aldrich) was distilled on calcium hydride just before use. Tetrahydrofuran was distilled on sodium/benzophenone just before use.

PPV was synthesized according to a procedure published elsewhere.[30] The obtained PPV polydispersity index (PID) was measured at 1.2 on gel permeation chromatography using polystyrene standards. The number-average molecular weight, $M_n$, and number of units ($n$) were determined by nuclear magnetic resonance (NMR) ($M_n = 4100$ g/mol, $n = 11$). PPV was dried by iterative azeotropic distillation in dried toluene just before use.

*sec*-Butyllithium was titrated before use. In a first step 1 mL of *sec*-butyllithium is added to 50 mL of water and titrated with 0.1 M sulfuric acid solution using phenolphatalein. The second step was conducted in a flamed flask under argon where 1 mL of *sec*-butyllithium reacts with an excess of dibromoethane. The reactive medium was quenched with water after 30 min and titrated with sulfuric acid. The first titration gives access to the concentration of *sec*-butyllithium and impurities, whereas the second one was only responsive to impurities, so that the concentration of active *sec*-butyllithium was easily determined. The *sec*-butyllithium used in the following was conditioned in a single bottle and was titrated at 1.4 M.

**GPC and NMR Characterizations**. $^1$NMR spectra were recorded on a Bruker 300 UltrashieldTM 300 MHz NMR spectrometer, with an internal lock on the 2H signal of the solvent ($CDCl_3$).

GPC measurements were performed at 60 °C in DMF with 0.5 g/L LiCl at a flow rate of 0.6 mL/mn using a Waters Alliance GPCV200 instrument equipped with triple detection. The elution column is a PSK-gel α.

**Morphological Investigation**. *Annealing Procedure.* A two-step thermal treatment was followed in order to erase the thermal history of the samples and to maintain the blend in the temperature region comprised between the glass transition temperature of P4VP, 140 °C, and the potential order−disorder transition temperature ($T_{ODT}$) of mesophases. Samples for morphological study were annealed in a high-vacuum oven ($5 \times 10^{-12}$ bar) for 2 h at 220 °C followed by 24 h at 160 °C. The morphologies yielded from this temperature annealing protocol were then compared with those obtained by isothermal annealing at (i) 160 °C for 48 h, (ii) 180 °C for 2 h, (iii) 200 °C for 2 h, and (iv) 220 °C for 2 h.

*Small- and Wide-Angle X-ray Scattering (SAXS and WAXS*). Small- and wide-angle X-ray scattering (SAXS, WAXS) diffractograms were acquired on an Anton-Paar SAXSess instrument. About 10 mg of blend was solvent-cast on a mica sheet and annealed. Temperature was regulated in situ up to 200 °C using a homemade sample holder. In the range 150−200 °C, a stable temperature was achieved in the middle of the sample holder after 30 min. All diffractograms at the various isothermal conditions were acquired after 1 h temperature equilibration.

*Small-Angle Neutron Scattering.* Samples for small-angle neutron scattering (SANS) were cast and annealed onto quartz substrates in the form of films whose thickness ranged between 30 and 50 μm and diameter was larger than 15 mm. SANS was performed at the Laue Langevin Institute on D11. Diffractogramms were acquired on a 64 × 64 cm CERCA 3He multidetector with sample−detector distance/collimation value set at 1.1 m/10.5 m, 4 m/4 m, and 10 m/10.5 m. The acquisition time depended on sample-to-detector distance and varied between 15 and 40 min. The wavelength was set at 4.51 Å, and the sample diaphragm diameter was 8 mm. Diffractograms have been superimposed to yield the full $q$ range spectrum.

*Ultramicrotomy.* All samples were embedded in a standard four components: epoxy resin (46 wt % Epon 812, 28 wt % (Dodecenyl Succinic Anhydride) DDSA, 25% (Nadic Methyl Anhydride) NMA, 1% (2,4,6-tris(dimethylaminomethyl) phenol) catalyst. In order to avoid diffusion of the resin components into the sample, the resin was precured 1 h 30 at 80 °C before embedding the sample. The sample was finally embedded in the precured epoxy resin, which was cured for 5 h at 70 °C. The samples were then ultramicrotomed on a Reichert-Jung microtome at room temperature. 50 nm thick sections were collected on 600 hexagonal mesh copper grids (EMS T601H-Cu). Staining of the P4VP phase was achieved by exposing collected sections to vapors of iodine for 1−3 h.

*Transmission Electron Microscopy (TEM).* Bright field imaging was performed on a CM100 Philips TEM operated at 80 kV (emission 2). All images were acquired on a SIS Morada CCD camera.

## Results and Discussion

**Synthesis**. Although synthesis of a PPV-*b*-polystyrene, has been previously achieved by atom transfer radical polymerization using a PPV macroiniatior,[9] this method proved to be not applicable to 4-vinylpyridine: the monomer competes with the ligand to complex the copper catalyst, potentially inducing low control over the reaction and thus polydisperse polymers. Moreover, the copper dopes the poly(vinylpyridine) block, producing a large number of quenching sites for excitons with consequent possible deleterious impact on photovoltaic properties of the material. PPV−P4VP block copolymer was thus synthesized following an anionic convergent route: well-defined aldehyde end-functionalized PPV was used as a quencher for the anionic polymerization of the 4-vinylpyridine (Scheme 1). To yield a pure copolymer despite the undesired chains deactivation occurring during synthesis and quenching, excess of P4VP living chains with respect to PPV quencher (3 mol equiv) was used. This procedure guarantees that the final material is PPV homopolymer free. The excess of P4VP was then removed by washing the sample with acidic water (pH = 3) in which the P4VP is protonated and thus soluble, while the block copolymer is not.

In a flamed round flask, 50 mL of distilled THF was cooled at −78 °C under argon. 0.65 mL (5.0 mmol) of freshly distilled

**Scheme 1. Steps Followed for the Convergent Synthesis of PPV-*b*-P4VP Copolymers**[a]

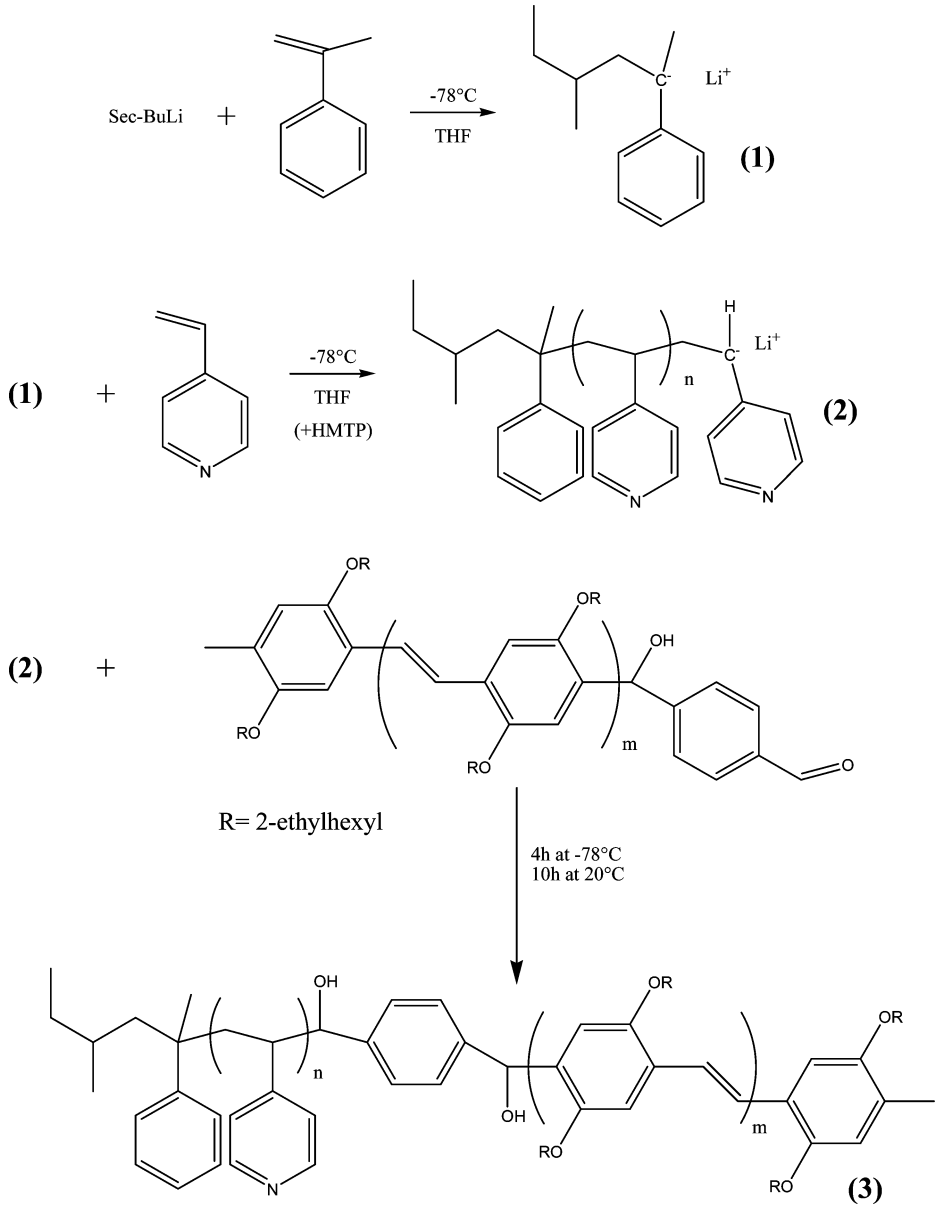


[a] The 4-vinylpyridine monomer is initiated with **1**, prepared in a separate step. To yield the final block copolymer, the poly(4-vinylpyridine) anion is quenched with the aldehyde derivative of the PPV.

α-methylstyrene was added. 1.4 M *sec*-butyllithium was added until persistent light red coloration is obtained. Then 1.78 mL (2.5 mmol) of 1.4 M *sec*-butyllithium was rapidly injected. The obtained initiator (number 1 in Scheme 1) proved to be stable for many hours when kept at −78 °C. This initiator has two advantages over *sec*-butyllithium: it is milder and colored. The former guarantees that the initiation will take place on the vinyl group without formation of secondary undesired products, whereas the latter permits to control the presence of the anions in the reactive medium and facilitate the rinsing procedure.

The anionic polymerization of 4-vinylpyridine was then carried out based on the procedure described by Varshney,[31] using lithium α-methylstyryl derivative (1) as initiator and THF with 1 vol % hexamethylphosphoric triamide (HMPT) as solvent for molecular weights larger than 5000 g/mol. This solution was preferred to the use of dimethylformamide because of the highly hygroscopic character of the latter. In a three-neck flask, 400 mL of freshly distilled THF (and possibly 1 mL HMTP) was cooled at −78 °C under argon. Initiator was added to the stirred solution until a persistent light red color was observed. Distilled 4-vinylpyridine was then added, inducing coloration loss due to the impurities introduced. Initiator was added rapidly until persistent yellow coloration was obtained. The required amount of initiator was then immediately injected. The polymerization was left running at −78 °C for 30 min.

PPV aldehyde end-functionalized quencher was dried by azeotropic distillation: it was dissolved in distilled toluene and evaporated at 50 °C under reduced pressure three times before being eventually dissolved in 10 mL of distilled toluene. This solution was then quickly injected into the reactive medium, which is kept at −78 °C for 4 h and left at room temperature over night. The solvent was then evaporated, and the obtained polymer was redissolved in 20 mL of dichloromethane. To separate the P4VP-*b*-PPV block copolymer from the P4VP homopolymer, the P4VP was protonated by washing three times the organic phase with 100 mL of pH = 3 chlorhydric acid aqueous solution and three times with 100 mL of water. The organic phase was washed three times with saturated hydrogen carbonate solution to recover the unprotonated water insoluble poly(vinylpyridine) block. After being washed with water, the

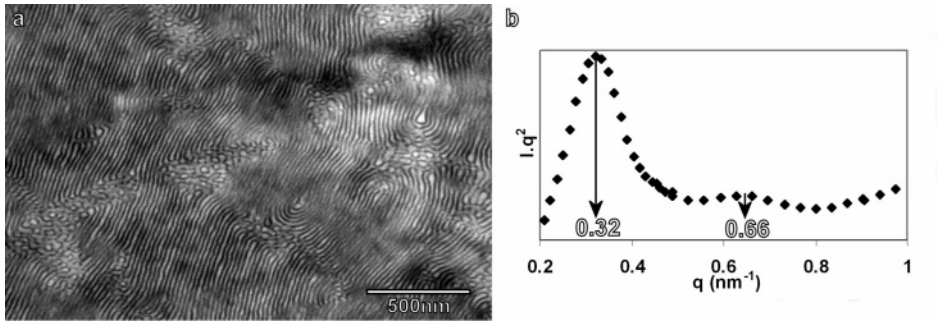


**Figure 1.** (a) Iodine-stained TEM micrographs showing long-range ordered lamellar structure in the P55 ($PPV_{11\ units}$−$P4VP_{51\ units}$) block copolymer. (b) Corresponding SANS diffractogram exhibiting the first- and second-order reflections of a lamellar phase with period 20 nm.

**Table 1. Summary of the Molecular Characterization for the Block Copolymer Considered**

| | | poly(*p*-phenylenevinylene) block[b] | | | poly(4-vinylpyridine) block[b] | | |
|---|---|---|---|---|---|---|---|
| | PDI[a] | no. of units | $M_n$ (g/mol) | overall vol fraction (%) | no. of units | $M_n$ (g/mol) | overall vol fraction (%) |
| P55 | 1.40 | 11 | 4100 | 45.1 | 51 | 5300 | 54.9 |
| P80 | 1.59 | 11 | 4100 | 19.2 | 173 | 18 300 | 80.8 |
| P88 | 1.30 | 11 | 4100 | 12.3 | 295 | 31 300 | 87.7 |

[a] Determined by GPC. [b] Determined by NMR.

organic phase was dried with $Na_2SO_4$ and evaporated to yield the pure PPV-*b*-P4VP homopolymer. The quenching efficiency was easily determined by NMR, as the aldehyde peak of the homoPPV appears at 10.2 ppm; because this peak disappears completely in the final purified block copolymers, it can be concluded that all block copolymers studied in the present work are completely free of homoPPV.

Because no universal calibration was performed on the GPC experiments, NMR was preferred for the determination of $M_n$: the respective sizes of PPV and PVP were determined by integrating P4VP H1 (6.4 ppm) and PPV H2 (4.0 ppm) peaks, respectively. The ratio of corresponding integrated area yields the ratio of both blocks molecular weights. By varying the relative molar amount of 4-vinylpyridine with respect to initiator, from 30 to 190, block copolymers with constant rod length and overall coil volume fraction of 55%($PPV_{4400g/mol}$−$P4VP_{5300g/mol}$), 80%($PPV_{4400g/mol}$−$P4VP_{18300g/mol}$), and 88%($PPV_{4400g/mol}$−$P4VP_{31300g/mol}$) (referred in what follows as P55, P80, and P88, respectively) were obtained. Volume fractions were calculated from mass fractions and densities of PPV and P4VP, 0.988 and 1.05 g/cm$^3$, respectively. GPC analysis revealed a monomodal distribution for all the block copolymer synthesized, indicating pure compounds, and polydispersity indexes (PDI) of 1.40, 1.59, and 1.30 were obtained for P55, P80, and P88, respectively. Table 1 summarizes the main findings in the characterization of the various block copolymer used.

**Morphologies and Self-Assembly Behavior.** The three different PPV-*b*-P4VP block copolymers studied in the present work have overall coil to rod volume fraction ranging from 55% to 88%, which, in the case of a coil−coil diblock copolymer, would lead to microphase separation into lamellar, hexagonal, and spherical phases provided that the driving force toward segregation, expressed by $\chi N$, is high enough. In the case of the present PPV-*b*-P4VP rod−coil system, the expected phase does not uniquely depend on the blocks volume ratio but also on the Maier−Saupe constant $\omega$, expressing the rod−rod steric repulsion. The balance of these two contributions, expressed by the ratio $\omega/\chi$, may lead to different morphologies for a fixed $\chi N$. For instance a large value of $\omega/\chi$ indicates a predominance of the liquid crystalline behavior over microphase separation and can drive a spherical or hexagonal phase into a lamellar smectic phase.[2] According to Landau expansion theory, in the volume fraction range of the block copolymers investigated in the present paper (0.55−0.88), for moderate to high tendency to segregation ($\chi N$ > 15−20) and intermediate Maier−Saupe interactions ($\omega/\chi$ < 4), isotropic, spherical, hexagonal, amorphous lamellar, or smectic lamellar phases can all be observed.[2] Additional experimental work suggests also other structures such as bicontinuous gyroid phases to be possible.[31]

The morphology characterization by small-angle X-ray scattering, small-angle neutron scattering, and transmission electron microscopy is performed on samples having undergone a two-step thermal annealing aimed at erasing the sample history and reaching thermodynamic equilibrium; the polymer is annealed at 220 °C for 2 h and then cooled to 160 °C. This temperature is then maintained for 24 h. During the first step, low viscosity and high chains mobility are expected, as confirmed by the fact that the polymer flows, permitting to quickly reach the equilibrium state. Successively, the sample is slowly cooled to 160 °C (at 0.5 °C/min). During the cooling and the second steps, the structure has time to relax and reach its new thermodynamically stable state at the lower temperature. The sample is finally cooled to the glass transition temperature of the poly(4-vinylpyridine) (140 °C), at which point it becomes a glassy solid whose morphology remains unchanged upon further cooling to room temperature. The morphologies observed using this thermal annealing protocol are then expected to be those thermodynamically stable just above the glass transition temperature of the poly(4-vinylpyridine). Figure 1a shows the TEM micrograph of the P55 sample after thermal annealing, presenting, as to be expected, a lamellar phase with a period of ca. 20 nm. The lamellar domains are organized in grains with sizes in the neighborhood of one to several microns. At grain boundaries, the morphology is highly distorted, showing bent PPV layers and closed loops. The lamellar phase is further confirmed by the SANS diffractogram shown in Figure 2b, in which two reflections are visible at $q_1 = 0.32$ nm$^{-1}$ and $q_2 = 0.66$ nm,[1] spaced as $q_1$:$q_2$ = 1:2, which is consistent with a lamellar phase of period 20 nm. Figure 2a shows the TEM micrograph of P80 sample. A short-range ordered hexagonal phase can be distinguished in which the PPV rods form the white, unstained cylindrical domains and the P4VP coils the continuous phase. In this case, grain domains are even smaller than in the P55 case, with highly distorted morphology in between grain

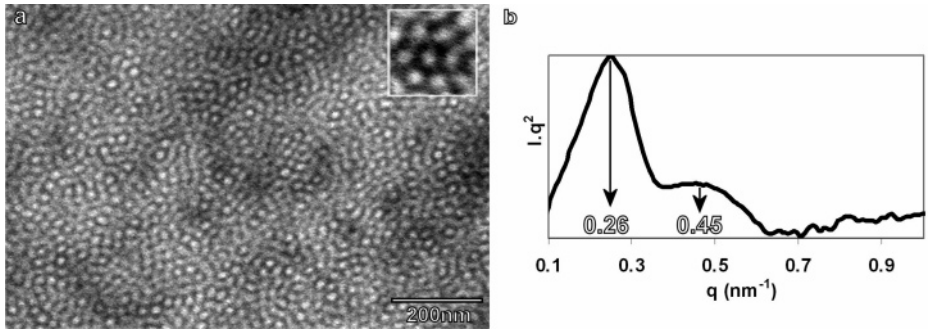


**Figure 2.** (a) Iodine-stained TEM micrographs of P80 ($PPV_{11\ units}$−$P4VP_{173\ units}$) block copolymer showing a short-range ordered hexagonal phase (inset shows 100 nm by 100 nm magnified picture). (b) Corresponding SAXS diffractogram exhibiting two peaks at $q_1 = 0.26$ nm$^{-1}$ and $q_2 = 0.45$ nm$^{-1}$ spaced as $q_1$:$q_2 = 1$:$\sqrt{3}$, confirming an hexagonal structure with lattice parameter $a = 28$ nm.

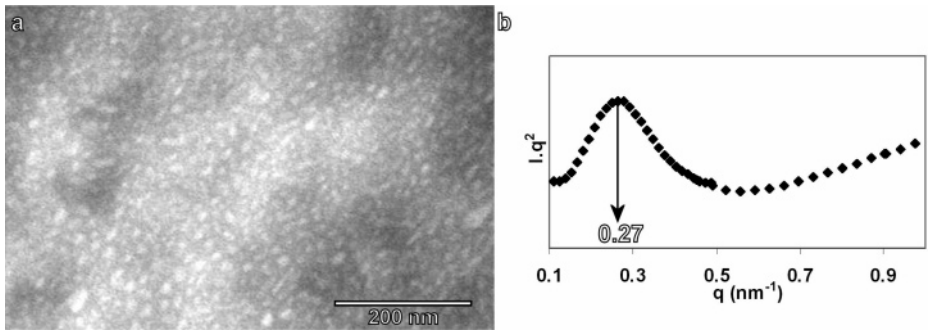


**Figure 3.** (a) Iodine-stained TEM micrograph showing a poorly ordered spherical phase morphology for P88 ($PPV_{11\ units}$−$P4VP_{295\ units}$) block copolymer. (b) The poor order of the spherical phase is confirmed by a single broad peak in the corresponding SANS diffractogram.

boundaries limiting the hexagonal order to few times the lattice parameter (see inset in Figure 2a). The corresponding SAXS diffractogram shown in Figure 2b also supports a hexagonal phase of 28 nm period, as it shows two reflections at $q_1 = 0.26$ nm$^{-1}$ and $q_2 = 0.45$ nm$^{-1}$, spaced as $q_1$:$q_2 = 1$:$\sqrt{3}$. The presence of this hexagonal phase at 20% rod volume fraction is consistent with predictions based on Landau expansion calculations.[2] Finally, the P88 sample exhibits a disordered spherical phase, as shown in Figure 3a, in which the minority PPV component forms the spherical domains and the P4VP blocks the continuous domains. The poor order apparent in the TEM micrograph of Figure 3a is confirmed by the corresponding SANS scattering, in which a single reflection peak at $q_1 = 0.27$ nm$^{-1}$ is visible. Although body-centered-cubic (bcc) spheres in rod−coil diblocks are predicted by Landau expansion in a narrow phase diagram region neighboring the hexagonal phase (and lower rod volume fractions), their experimental observation is uncommon.

The PPV rods packing mechanisms within lamellar, hexagonal, and spherical domains were investigated by WAXS. Among the three block copolymers, only the P55 with lamellar morphology exhibits the characteristic peak at $q_1 = 6.5$ nm$^{-1}$ expressing liquid crystalline-mediated close packing of PPV rods. For this latter sample, the WAXS signal is reported after various thermal annealing protocols in Figure 4. For samples having followed the standard two-step annealing process (curve a), a second reflection at $q_2 = 13$ nm$^{-1}$ appears, indicative of very efficient packing. Systems annealed at 160 °C (curve b), on the other end, show only the first peak and this is broader than for samples having followed a two-step annealing. Finally, samples heated up to 180 °C do not show any peak, as a result of the disruption of liquid crystalline interactions and melting of rod−rod close packing order (curve c). It should be noted, however, that in this case the peak is reversibly recovered upon cooling the system to 160 °C or below. These results indicate that for P55 samples properly annealed the PPV rods are closely

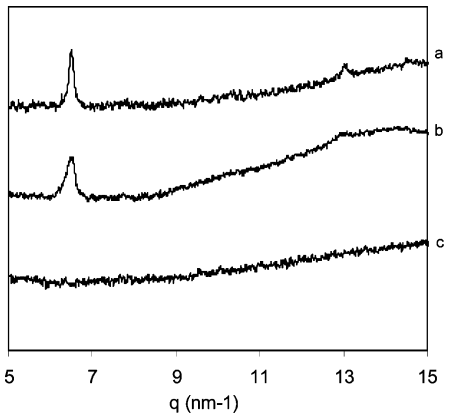


**Figure 4.** WAXS diffractogramm acquired on P55 after separate annealing in high-vacuum ovens at (a) 220 °C for 2 h and then 160 °C for 12 h and slowly cooled, (b) 160 °C for 48 h and slowly cooled, and (c) acquired at 180 °C. The loss of the inter-rods interaction peak at 180 °C indicates the disruption of liquid crystalline interactions and melting of the smectic order. If the sample undergoes annealing at 160 °C, a single peak at $q_1 = 6.5$ nm$^{-1}$ appears, indicative of a liquid crystalline interaction-driven close-packing. Upon annealing sample at 220 °C first followed by slow cooling and postannealing at 160 °C, two peaks at $q_1 = 6.5$ nm$^{-1}$ and $q_2 = 13$ nm$^{-1}$ ($q_1$:$q_2 = 1$:2) appear, indicative of restoration of close packing between rods and improved smectic order.

packed within the corresponding domains, forming a smectic lamellar phase.

Then, four different molecular organizations can be envisaged for the P55 smectic lamellar organization: smectic $A_1$, $A_2$, $C_1$, or $C_2$, respectively corresponding to untilted monolayer, untilted double layer, tilted monolayer, and tilted bilayer. To determine which model suitably describes the structure observed, the PPV lamellae width is easily calculated by multiplying the lattice period obtained by SANS by the PPV volume fraction. Following this simple route, the PPV lamellae width was determined at 8.8 nm. On the basis of molecular simulations,

the PPV rod length for a chain containing 11 units is expected to be 7.26 nm.[9] The lamellae width is thus larger than the contour length, implying that the molecular organization of the lamellae is not a monolayer but a tilted double layer ($SmC_2$). The tilt angle is then easily calculated from simple geometrical considerations. Its value, 52.4°, is very close to the one previously determined (53.7°) in polystyrene−PPV clusters.[9] In that work, it was demonstrated indeed that the affordable tilting angles for PPV smectic domains are constrained to a discrete set of values to enhance overlapping of the $\pi$-orbitals, yielding the observed $\pi-\pi$ inter-rod interactions. The similar tilt angle and the presence of a peak on the WAXS diffractogramm at 6.5 $nm^{-1}$ for both polystyrene−PPV and P4VP−PPV block copolymers support that both structures have the same organization at the molecular level and are stabilized by intermolecular $\pi-\pi$ interactions.

The lack of inter-rod liquid crystalline order peak is also very informative in the other two block copolymer morphologies. Indeed, while close packing of PPV rods in spheres cannot be achieved, this is still attainable in hexagonal packing, as both homeotropic and isotropic orientation of the rod are possible. In the first case, rods are aligned orthogonally to and emanating radially with respect to the cylinder axis, while in the second case they are aligned parallel to the cylinders.[32]

Similarly to the lamellar phase, also in the hexagonal PPV cylinder radius ($r$) can easily be determined from the lattice period and blocks volume fractions:

$$r = a\sqrt{\frac{\sqrt{3}}{2}\frac{\phi_{PPV}}{\pi}} = 6.5 \text{ nm}$$

where $a$ is the lattice parameter and $\varphi_{PPV}$ the overall PPV volume fraction in the copolymer (i.e., 19.2% for P80).

This value is about 10% off to the contour length of a single rod (7.26 nm), which is in strong support of the hypothesis of a homeotropic PPV packing. Indeed, an isotropic packing would imply that PPV molecules are stacked along a common director with inter-rod liquid crystalline and $\pi-\pi$ interactions, which is not observed on P80 WAXS diffractograms. This also indicates that the PPV rods are aligned in such a way that each plane containing a PPV molecule is passing by the cylinder axis. This inhibits liquid crystalline order and $\pi$-orbitals stacking among contiguous PPV rods, in accordance with experimental WAXS evidence.

On the basis of the arguments developed above, the molecular models for packing of PPV rods in the corresponding domains of the P55 smectic lamellar phase and P80 columnar hexagonal phase are sketched in Figure 5.

Since the liquid crystalline interactions vanish at 180 °C, as demonstrated in Figure 4, we have investigated the effect of different annealing temperature protocols on the microstructure of P55. The $T_{ODT}$ for this system is observed between 200 and 220 °C by TEM on samples quenched by liquid nitrogen. Thus, P55 undergoes two main order−disorder transitions with temperature, at two different length scales, e.g., the rod−rod interdistance and the lamellar period. First, at 180 °C an order−disorder transition is observed within PPV domains, associated with the vanishing rod−rod interactions and melting of rods close packed ordering. The existence of the temperature-induced smectic-in-lamellar to lamellar transition, $T_{SL}$, is predicted by Landau expansion theories.[2] Second, a more classical order−disorder transition temperature, $T_{ODT}$, is observed at 210 °C, and it is associated with the melting of the lamellar phase into a fully homogeneous block copolymer isotropic fluid. The

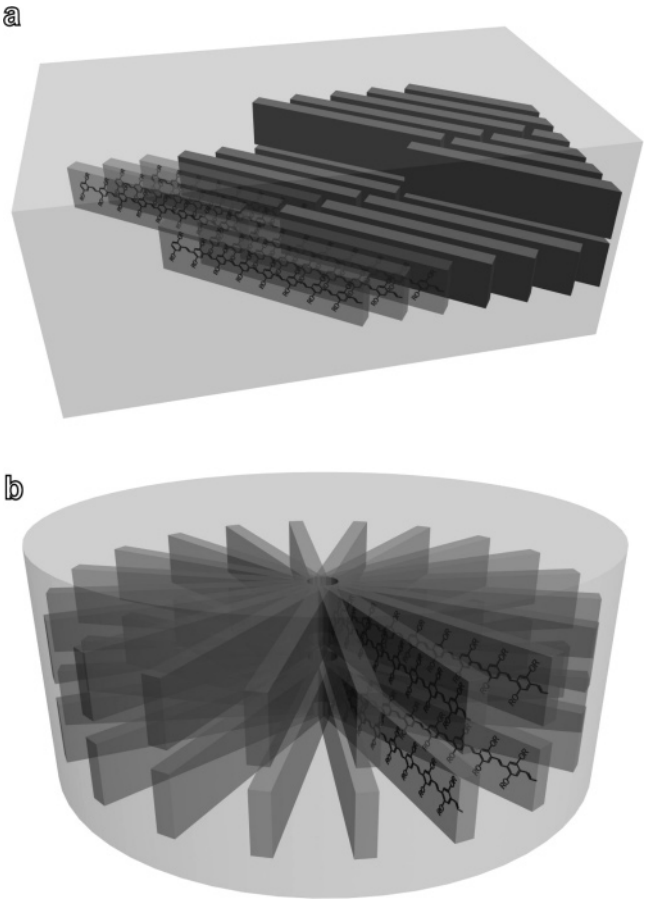


**Figure 5.** Molecular models proposed for packing of PPV rods in lamellar and hexagonal phases. (a) In the case of P55, rods organize in a Smectic C2 arrangement with a tilt angle of 52°, allowing close packing of PPV units in contiguous rods, and $\pi-\pi$ interactions among rods. (b) In the case of P80, rods organize within cylinders in a homeotropic arrangement, oriented radially and perpendicular to cylinder axis. Because of the lack of an inter-rods interactions peak in the WAXS diffractogram, the planes containing PPV rods are expected to orient parallel to cylinder axis.

consequences of the interplay of these two phenomena are shown in Figure 6: TEM images have been acquired on bulk samples slowly evaporated from dichloromethane and then annealed or quenched at different temperatures. All samples exhibit a clear lamellar morphology with similar period but significant variation in the lamellae long-range order and persistence length. The sample annealed at 160 °C (Figure 6 a) for 48 h presents lamellar-like structure; nevertheless, domains are only coherent over few hundredths of nanometers. This short-range order is the result of competing liquid crystallinity and microphase segregation. However, this coherence length is subsequently increased when the P55 samples are annealed for 2 h at 180 °C (b) or 200 °C (c), that is, when $T_{SL} < T < T_{ODT}$, where it reaches more than 1 $\mu$m. Further increase of temperature brings the system above $T_{ODT}$ and induces the melting of the lamellar structure (d). Very illustrative is the structure arising in the sample undergoing a two steps annealing; 2 h at 220 °C, slowly cooled to 160 °C, and maintained 12 h at 160 °C (Figure 6e), as it shows lamellar order globally aligned over 10 $\mu$m. The difference between simple annealing at 160 °C and the two steps procedure is remarkable and is due to the fact that lamellar phase can form without interfering liquid crystalline interactions when $T_{SL} < T < T_{ODT}$. Once a fine lamellar structure is achieved in this temperature range, the system can be cooled at $T < T_{SL}$ to regain rod−rod interactions-mediated rod close packing, while preserving the long-range lamellar order. The liquid crystalline

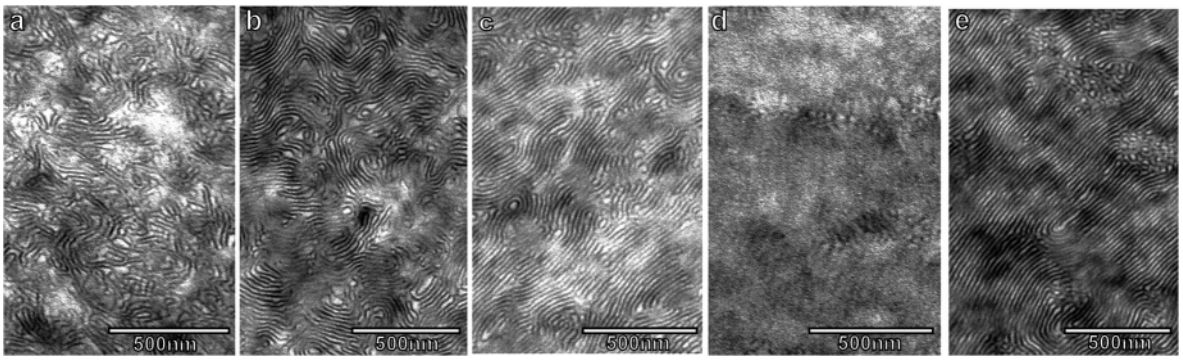


**Figure 6.** Representative iodine-stained TEM micrographs for P55 with different thermal history: (a) 160 °C for 48 h and slowly cooled, (b) 180 °C for 2 h and quenched, (c) 200 °C for 2 h and quenched, (d) 220 °C for 2 h and quenched, and (e) 220 °C for 2 h, slowly cooled to 160 °C, maintained at 160 °C for 12 h, and slowly cooled. The structure order range is increasing from (a) to (c) whereas it is completely disappearing at 220 °C. Melting at 220 °C and slow cooling to 160 °C proved to promote the formation of a long-range order lamellar structure (e).

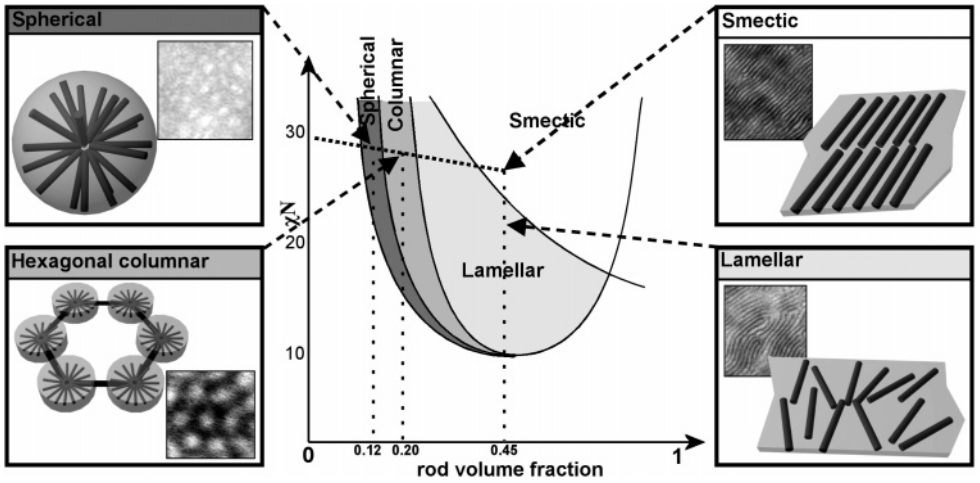


**Figure 7.** Comparison between the phase diagram predicted by Landau expansion theories for rod−coil block copolymers and the microphase-separated morphologies experimentally observed for PPV−P4VP block copolymers. The theoretical phase diagram is redrawn from ref 2.

ordering recovered during this last step could have an influence on the photovoltaic properties of the material[33] due to different diffusivity of excitons in smectic or amorphous lamellar domains. The transitions form smectic to lamellar as well as the hexagonal and spherical morphologies reported in the present paper are fully predicted by Landau expansion theory. This remarkable consistency between experiments and theoretical predictions is sketched in Figure 7.

## Conclusions

The synthesis and self-assembly behavior of poly(diethylhexyloxy-*p*-phenylenevinylene)-*b*-poly(4-vinylpyridine) rod−coil block copolymers with molecular weight between 5000 g/mol and 30000 g/mol, and coil volume fraction between 55% and 88% have been described. These polymers exhibit lamellar, hexagonal and spherical microphase separated morphologies when going from high to low rod volume fraction, respectively. Furthermore, while for the hexagonal and spherical phases wide-angle X-rays scattering shows no evidence of rods close packing, in the case of the lamellar phase evidence of rod−rod interactions inducing rod packing with 1 nm periodicity appears for temperature lower than 180 °C. This demonstrates that both smectic-in-lamellar and lamellar phases are possible, respectively below and above 180 °C, which is the consequence of liquid crystalline interactions among PPV rods. These interactions can be cancelled at high temperature, letting the system to self-assemble based solely on micro segregation driving force. Thus, two order−disorder transition temperatures are observed for the symmetric PPV-b-P4VP block copolymer: at lower temperatures (180 °C) a smectic-in-lamellar to lamellar transition is observed, and at higher temperature (210 °C) a lamellar to isotropic phase transition. On the morphologies of the lamellar phase, the effect of coexistence of liquid crystalline interactions and tendency to microphase separation leads, at temperatures lower than 180 °C, to a smectic lamellar phase with short-range order, while, at temperatures higher than 180 °C, a long-range order lamellar phase is obtained. Remarkably, for spherical and hexagonal lamellar phases, for which close packing of rods do not apply, different temperature annealing protocols have no influence on the final morphology. The spherical, hexagonal and lamellar phases, as well as the smectic-in-lamellar to lamellar order−disorder transition temperature are well predicted by Landau expansion theories.

On the basis of volume fraction and lattice parameters values, as well as evidence of rod−rod close packing, molecular models for the lamellar and hexagonal phase were proposed. The lamellar phase appears to be organized as a smectic C bilayer with tilt angle of 52°, which allows minimum distance between PPV monomer units and $\pi-\pi$ interactions between contiguous PPV blocks, while the hexagonal phase is expected to be organized in a homeotropic configuration in which PPV rods orient radially and perpendicular to cylinder axis, and the P4VP coils form the continuous phase.

**Acknowledgment.** The authors acknowledge the Swiss Science National Foundation, BASF Aktiengesellschaft, and Gebert ruf Stiftung for financial support. The authors kindly

acknowledge Dr. Peter Lindner for support during SANS measurements, Dr. Tuan Nguyen, and Mr. Philippe Charpilloz for GPC characterization. N.S. thanks Dr. Nicolas Leclerc (LIPHT) for useful discussions.

## References and Notes

(1) Semenov, A. N. *Mol. Cryst. Liq. Cryst.* **1991**, *209*, 191−199.
(2) Reenders, M.; ten Brinke, G. *Macromolecules* **2002**, *35*, 3266−3280.
(3) Matsen, M. W.; Barrett, C. *J. Chem. Phys.* **1998**, *109*, 4108−4118.
(4) Leibler, L. *Macromolecules* **1980**, *13*, 1602−1617.
(5) Bates, F. S.; Fredrickson, G. H. *Annu. Rev. Phys. Chem.* **1990**, *41*, 525−557.
(6) Bates, F. S.; Fredrickson, G. H. *Phys. Today* **1999**, *52*, 32−38.
(7) Pryamitsyn, V.; Ganesan, V. *J. Chem. Phys.* **2004**, *120*, 5824−5838.
(8) Duchs, D.; Sullivan, D. E. *J. Phys.: Condens. Matter* **2002**, *14*, 12189−12202.
(9) Sary, N.; Mezzenga, R.; Brochon, C.; Hadziioannou, G.; Ruokolainen, J. *Macromolecules* **2007**, *40*, 3277−3286.
(10) Yamamoto, T.; Komarudin, D.; Arai, M.; Lee, B. L.; Suganuma, H.; Asakawa, N.; Inoue, Y.; Kubota, K.; Sasaki, S.; Fukuda, T.; Matsuda, H. *J. Am. Chem. Soc.* **1998**, *120*, 2047−2058.
(11) Yamamoto, T.; Suganuma, H.; Maruyama, T.; Inoue, T.; Muramatsu, Y.; Arai, M.; Komarudin, D.; Ooba, N.; Tomaru, S.; Sasaki, S.; Kubota, K. *Chem. Mater.* **1997**, *9*, 1217−1225.
(12) Friedel, P.; John, A.; Pospiech, D.; Jehnichen, D.; Netz, R. R. *Macromol. Theory Simul.* **2002**, *11*, 785−793.
(13) de Boer, B.; Stalmach, U.; van Hutten, P. F.; Melzer, C.; Krasnikov, V. V.; Hadziioannou, G. *Polymer* **2001**, *42*, 9097−9109.
(14) Segalman, R. A., Brochon, C., Hadziioannou, G., Sun, S.-S., Sariciftci, N. S., Eds.; Taylor & Francis: London, 2005; p 403.
(15) van der Veen, M. H.; de Boer, B.; Stalmach, U.; van de wetering, K. I.; Hadziioannou, G. *Macromolecules* **2004**, *37*, 3673−3684.
(16) Li, W. J.; Wang, H. B.; Yu, L. P.; Morkved, T. L.; Jaeger, H. M. *Macromolecules* **1999**, *32*, 3034−3044.
(17) Tew, G. N.; Pralle, M. U.; Stupp, S. I. *J. Am. Chem. Soc.* **1999**, *121*, 9852−9866.
(18) Olsen, B. D.; Segalman, R. A. *Macromolecules* **2005**, *38*, 10127−10137.
(19) Marsitzky, D.; Brand, T.; Geerts, Y.; Klapper, M.; Mullen, K. *Macromol. Rapid Commun.* **1998**, *19*, 385−389.
(20) Francke, V.; Rader, H. J.; Geerts, Y.; Mullen, K. *Macromol. Rapid Commun.* **1998**, *19*, 275−281.
(21) Hempenius, M. A.; Langeveld-Voss, B. M. W.; van Haare, J.; Janssen, R. A. J.; Sheiko, S. S.; Spatz, J. P.; Moller, M.; Meijer, E. W. *J. Am. Chem. Soc.* **1998**, *120*, 2798−2804.
(22) Kukula, H.; Ziener, U.; Schops, M.; Godt, A. *Macromolecules* **1998**, *31*, 5160−5163.
(23) Wang, H. B.; Wang, H. H.; Urban, V. S.; Littrell, K. C.; Thiyagarajan, P.; Yu, L. P. *J. Am. Chem. Soc.* **2000**, *122*, 6855−6861.
(24) Leclere, P.; Parente, V.; Bredas, J. L.; Francois, B.; Lazzaroni, R. *Chem. Mater.* **1998**, *10*, 4010−4014.
(25) Friend, R. H.; Gymer, R. W.; Holmes, A. B.; Burroughes, J. H.; Marks, R. N.; Taliani, C.; Bradley, D. D. C.; Dos Santos, D. A.; Bredas, J. L.; Logdlund, M.; Salaneck, W. R. *Nature (London)* **1999**, *397*, 121−128.
(26) Laiho, A.; Ras, R. H. A.; Valkama, S.; Ruokolainen, J.; Osterbacka, R.; Ikkala, O. *Macromolecules* **2006**, *39*, 7648−7653.
(27) Heeger, A. J. *Rev. Mod. Phys.* **2001**, *73*, 681−700.
(28) Radzilowski, L. H.; Stupp, S. I. *Macromolecules* **1994**, *27*, 7747−7753.
(29) Lee, M.; Cho, B. K.; Jang, Y. G.; Zin, W. C. *J. Am. Chem. Soc.* **2000**, *122*, 7449−7455.
(30) Stalmach, U.; de Boer, B.; Post, A. D.; van Hutten, P. F.; Hadziioannou, G. *Angew. Chem., Int. Ed.* **2001**, *40*, 428−430.
(31) Lee, M.; Cho, B. K.; Kang, Y. S.; Zin, W. C. *Macromolecules* **1999**, *32*, 7688−7691.
(32) Mao, G. P.; Wang, J. G.; Clingman, S. R.; Ober, C. K.; Chen, J. T.; Thomas, E. L. *Macromolecules* **1997**, *30*, 2556−2567.
(33) Samuel, I. D. W.; Rumbles, G.; Collison, C. J. *Phys. Rev. B* **1995**, *52*, 11573−11576.